Mode-locking in Coupled Map Lattices

R. Carretero-González* †, D.K. Arrowsmith and F. Vivaldi
School of Mathematical Sciences, Queen Mary and Westfield College, Mile End Road, London E1 4NS, U.K.
(Physica D **103** (1997) 381–403)

Keywords: Coupled map lattices, travelling waves, mode-locking, symbolic dynamics.

We study propagation of pulses along one-way coupled map lattices, which originate from the transition between two superstable states of the local map. The velocity of the pulses exhibits a staircase-like behaviour as the coupling parameter is varied. For a piece-wise linear local map, we prove that the velocity of the wave has a Devil's staircase dependence on the coupling parameter. A wave travelling with rational velocity is found to be stable to parametric perturbations in a manner akin to rational mode-locking for circle maps. We provide evidence that mode-locking is also present for a broader range of maps and couplings.

1. INTRODUCTION

An interesting feature of coupled map lattices (CML) [1,2] is the widespread occurrence of the so-called *spatio-temporal chaos* [3,4], which is irregular behaviour in time as well as space. Equally interesting is the appearance of coherent structures from an apparently decorrelated medium [5]–[7]. For example, an interface separating two different phases may travel along the lattice [8]–[11]. The movement of such a front depends on the strength of the coupling between lattice sites. This paper is concerned with investigating some aspects of this phenomenon.

We consider an infinite collection of cells with a local dynamical variable $x_t(i)$, characterizing the state of the i-th cell at time t. Both i and t are integer. The global state of the lattice at time t is given by the state vector

$$X_t = \{x_t(i)\} = (\ldots, x_t(i-1), x_t(i), x_t(i+1), \ldots). \quad (1)$$

The state of the i-th cell at time $t+1$ given by

$$x_{t+1}(i) = F_i(\ldots, x_t(i-1), x_t(i), x_t(i+1), \ldots), \quad (2)$$

where the function F_i is determined by the local dynamics in each cell as well as the interaction between cells. A physically meaningful interaction will have typically a limited range, with decreasing strength for distant neighbours. Equation (2) defines the components of the global map F:

$$F = (\ldots, F_{-1}, F_0, F_1, \ldots) \qquad X_{t+1} = F(X_t).$$

A mapping of global states that will be of use in the following is the *shift mapping*

$$G(\{x_t(i)\}) = \{x_t(i+1)\}. \quad (3)$$

It should be clear that F and G commute.

We consider *homogeneous* CML (same map F_i for all cells) with linear nearest-neighbours interaction. The two most widely used models are

$$x_{t+1}(i) = (1-\varepsilon) f(x_t(i)) + \frac{\varepsilon}{2}\left(f(x_t(i-1)) + f(x_t(i+1))\right) \quad (4)$$

and

$$x_{t+1}(i) = (1-\varepsilon) f(x_t(i)) + \varepsilon f(x_t(i-1)), \quad (5)$$

which are called *diffusive* and *one-way* CML respectively. The coupling strength ε (also called the *diffusive parameter*) satisfies $0 \le \varepsilon \le 1$ to ensure the conservation of flux between neighbouring sites.

In this paper we consider the propagation of localized wavefronts along a linear one-way CML. Localized states and step states (localized wavefronts) are introduced in the next section, where we establish some of their basic properties. In section 3 we introduce a one-parameter family of piece-wise linear local maps, for which wavefronts can propagate coherently in a simple way. In the following section we show that the dynamics of an important class of wavefronts can be reduced to the study of a discontinuous piecewise-linear circle map, depending on two parameters. We study this family with methods of symbolic dynamics. These results are then applied to the pulse propagation in section 5. We show that for each value of the parameters the velocity of the pulse is well-defined, and we use it to characterize the structure of the parameter space. The latter is found to be structurally similar to that of a subcritical circle map, with velocity playing the role of rotation number. We establish the occurrence of a critical transition from a stable standing signal to a stable travelling one, as the coupling parameter is increased, and we prove parametric stability of pulses travelling with rational velocity. The velocity of the travelling pulse is found to have Devil's staircase-like

*e-mail: R.Carretero@ucl.ac.uk
†New address: Center for Nonlinear Dynamics and its Applications (CNDA), Dept. Civil and Environmental Engineering, University College London, Gower Street, LONDON WC1E 6BT

dependence on the coupling parameter (see figure 1). In the last section we indicate how to generalize our results to a broader range of functions and couplings.

2. LOCALIZED STATES AND PROPAGATING FRONTS

We first define localized states, step states and their velocity of propagation and then establish some of their basic properties. In what follows, we deal with a linear one-way CML, unless stated otherwise.

1. Localized states and step states

Let $\Delta x_t(i) = |x_t(i+1) - x_t(i)|$. The *mass* $M(X_t)$ of a global state X_t is defined as the variation of the local states

$$M_t = M(X_t) = \sum_{i=-\infty}^{\infty} \Delta x_t(i).$$

We restrict our attention to states with positive finite mass (a zero-mass state is a uniform state).

For each lattice site $i \in \mathbb{Z}$ we define the probability

$$p_t(i) \;=\; \frac{\Delta x_t(i)}{M_t}. \tag{6}$$

The mean μ and the variance σ of the variable i with respect to the probability distribution (6) are given by

$$\mu_t = \mu(X_t) = \sum_{i=-\infty}^{\infty} i\, p_t(i)$$
$$\sigma_t^2 = \sigma(X_t)^2 = \sum_{i=-\infty}^{\infty} (i-\mu_t)^2\, p_t(i).$$

The quantity μ_t is called *centre of mass* of the state X_t, and σ_t its *width*. The centre of mass and the width give, respectively, the average position and spread of the localized state.

A state X_t with finite centre of mass and width is said to be *localized*. If, in addition, there exists a positive constant $\kappa < 1$ such that $\Delta x_t(i) = O(\kappa^{|i|})$, then the state is *exponentially localized*. For an exponentially localized state, not only the mean and variance exist, but also all central moments of the distribution (6).

We are interested in localized states that can model wavefronts. So we define a *step state* to be a localized state for which the configuration $\{x_t(i)\}$ is asymptotic, for $i \to \pm\infty$, to two distinct fixed points of f [12]:

$$\lim_{i\to\pm\infty} x_t(i) = x_\pm^*; \qquad f(x_\pm^*) = x_\pm^*. \tag{7}$$

The mass of a step state is bounded from below

$$M(X_t) \geq \Delta x^* = |x_+^* - x_-^*|. \tag{8}$$

The simplest such state is a *pure step state*, that is, a step function between the two fixed points

$$P(k) \equiv x_t(i) = \begin{cases} x_-^* & \text{if} \quad i \leq k \\ x_+^* & \text{if} \quad i > k. \end{cases} \tag{9}$$

For this pure state $\mu(P(k)) = k$ and $\sigma(P(k)) = 0$.

A step state has *minimal mass* or *minimal variation*, *i.e.* $M(x_t) = \Delta x^*$ (cf. (8)), if and only if its local states are ordered, that is if $x_t(i) \leq x_t(i+1)$ when $x_-^* < x_+^*$ (or $x_t(i) \geq x_t(i+1)$ when $x_-^* > x_+^*$) for all i. It is plain that if the configuration of the one-way CML has minimal mass at time t it is going to preserve its minimal mass at any time greater than t provided that f is a non-decreasing function if $x_-^* < x_+^*$ and non-increasing if $x_-^* > x_+^*$.

The global dynamics causes centre of mass and width of a localized state to evolve. In this respect, two points need consideration. Firstly, the existence of the probability p_t does not automatically imply that of p_{t+1}, and secondly, the image of a localized state is not necessarily localized. To achieve the above conditions, we impose some mild restrictions on the local map f as well as the state X_t. The importance of the states defined above is that they are invariant under the dynamics of the CML — for the complete statements and proofs see appendix A. This gives the framework for the existence of steady step states and travelling ones.

2. Travelling velocity and basic properties

From the previous definitions and results it is clear that if the initial state X_0 is a step state, then $\mu(X_t)$ and $\sigma(X_t)$ are defined for all $t \geq 0$ (see appendix A for details). Our main interest is to determine the average velocity v of the centre of mass along a global orbit, namely

$$v \;=\; v(\varepsilon, X_0) \;=\; \lim_{t\to\infty} \frac{1}{t}(\mu_t - \mu_0).$$

A formal analysis on the stability of exponentially localized step states establishes the following quite general property of the velocity of a step state in one-way CML:

Theorem 1. *Let X_0 be an exponentially localized step state of a one-way CML. Let the local map f be bounded, and let f be a contraction mapping in a neighbourhood of the fixed points* (7). *Then, for all sufficiently small ε, $v(\varepsilon) = 0$ and $v(1-\varepsilon) = 1$, independently of X_0.*

The proof of this theorem is given in appendix A. The condition that f be a contraction mapping is a bit stronger than the condition that $x^*_\pm$ be attracting. We shall see that for an initial localized interface of the type (9), the critical behaviour is much richer than a discontinuous transition from $v=0$ to $v=1$, at some intermediate value of ε. Rather, the dependence of v on ε is characterized by infinitely many critical values, in correspondence to the boundaries of intervals in ε, where the velocity is a given rational number (see figure 1).

A general feature of the velocity of the travelling wave is its symmetry. Let us define $\delta = 1-\varepsilon$ and consider a moving reference frame with a unit positive velocity:

$$\begin{cases} y_t(i) &=& x_t(i) \\ y_{t+1}(i) &=& x_{t+1}(i+1) \\ \vdots & & \vdots \\ y_{t+k}(i) &=& x_{t+k}(i+k). \end{cases}$$

The one-way CML in the moving frame now reads

$$\begin{array}{rcl} y_{t+1}(i-1) &=& \delta f(y_t(i)) + (1-\delta) f(y_t(i-1)) \\ \Longrightarrow \quad y_{t+1}(i) &=& (1-\delta) f(y_t(i)) + \delta f(y_t(i+1)). \end{array} \tag{10}$$

Equation (10) represents a one-way CML of the type (5) but coupled in the opposite direction. Thus, taking into account the moving reference frame and the definition of δ we can conclude that

$$1 - v(\varepsilon) = v(1-\varepsilon). \tag{11}$$

Therefore the velocity of the travelling wave in a one-way CML of the form (5) is symmetric with respect to the point $(\varepsilon, v(\varepsilon)) = (1/2, 1/2)$ (see figure 1). This important symmetric property allows one to restrict the study of the velocity to the ε-interval $[0, 1/2]$.

3. A PIECE-WISE LINEAR LOCAL MAP

In this section we deal with the coherent propagation of a wavefront (without damping or dispersion) along the lattice. We confine our attention to states with minimal mass. In order to ensure that this property is preserved under iteration, we shall require the local map f to be non-decreasing as stated before. In addition, we ask f to be continuous and to have two stable fixed points x^*_- and x^*_+ (with $x^*_- < x^*_+$). So f will have precisely one unstable fixed point at x^* with $x^*_- < x^* < x^*_+$. The local dynamics takes place on the interval $I = [x^*_-, x^*_+]$, where there are two basins of attraction $I_- = [x^*_-, x^*)$ and $I_+ = (x^*, x^*_+]$ for the fixed points x^*_- and x^*_+, respectively.

1. The local mapping

A simple one-parameter family of maps that fulfills the above requirement is given by (see figure 2)

$$f_a(x) = \begin{cases} -1 & \text{if } x \le -a \\ \frac{1}{a} x & \text{if } -a < x < a \\ 1 & \text{if } x \ge a \end{cases} \qquad 0 < a < 1, \tag{12}$$

and by the step function between -1 and 1 centered at the origin when $a=0$. The fixed points $x^*_- = -1$ and $x^*_+ = 1$ are superstable, with basins $I_- = [-1, 0)$ and $I_+ = (0, 1]$, respectively. The repeller is the origin $x^* = 0$. The coupled map lattice now depends on the two parameters ε and a, and the parameter space is the unit square. The one-way CML with local mapping f_a and coupling ε will be denoted by $F_{\varepsilon,a}$.

We partition the interval $I = [-1, 1]$ into the unstable domain $U = (-a, a)$ and the superstable domains $S_- = [-1, -a]$ and $S_+ = [a, 1]$. Any site falling within $S_\pm$ maps, under f_a, to $x^*_\pm$ at the next iteration.

We begin considering states of minimal mass X_t whose configurations $\{x_t(i)\}$ form a *non-decreasing* sequence. Because X_t is a localized state, only a finite number n of local states belong to U:

$$i \in \{k+1, \ldots, k+n\} \quad \Longleftrightarrow \quad x_t(i) \in U. \tag{13}$$

For $i \le k$ $(i > k+n)$, the local states belong to the superstable domain S_- (S_+) and their image under f_a is -1 $(+1)$. Consequently, if we let X'_t be the state obtained from X_t by replacing $x_t(i)$ with -1 for $i \le k$ and with $+1$ for $i > k+n$, then $F_{\varepsilon,a}(X_t) = F_{\varepsilon,a}(X'_t)$. The state X'_t is the *reduced state* associated with X_t, and we write $X_t \sim X'_t$. We will reduce all states after each iteration of the mapping $F_{\varepsilon,a}$.

So, without loss of generality, we shall restrict our attention to states of the type

$$X_t = (\ldots, -1, -1, x_t(k+1), \ldots, x_t(k+n), 1, 1, \ldots) \quad \text{with} \quad |x_t(i)| < a, \quad i = k+1, \ldots, k+n.$$

The number n of local states in U is called the *size* of X_t. The knowledge of the range (13) provides useful information about position and width of a step state. Indeed the center of mass of X_t satisfies the bounds

$$k + \frac{n(1-a)}{2} < \mu(X_t) < (k+n) - \frac{n(1-a)}{2} \tag{14}$$

and the width

$$\frac{n(1-a)}{2} < \sigma(X_t) < \frac{n}{2}. \tag{15}$$

The image of X_t is

$$\begin{array}{rcl} X_{t+1} &=& (\ldots, -1, -1, f_-(x_t(k+1)), \ldots, \\ & & x_{t+1}(k+n), f_+(x_t(k+n)), 1, \ldots) \end{array}$$

where

$$
\begin{aligned}
f_-(x) &= \frac{1-\varepsilon}{a}\,x - \varepsilon \\
f_+(x) &= \frac{\varepsilon}{a}\,x + (1-\varepsilon).
\end{aligned}
\tag{16}
$$

X_{t+1} has at most $n+1$ sites in U. The reduced state X'_{t+1} is one of the following:

$$
\begin{array}{llll}
(a) & (\ldots,-1,-1, & x_{t+1}(k+1), & x_{t+1}(k+2),\ldots, \\
 & x_{t+1}(k+n), & 1, & 1,\ldots) \\
(b) & (\ldots,-1,-1, & -1, & x_{t+1}(k+2),\ldots, \\
 & x_{t+1}(k+n), & x_{t+1}(k+n+1), & 1,\ldots) \\
(c) & (\ldots,-1,-1, & x_{t+1}(k+1), & x_{t+1}(k+2),\ldots, \\
 & x_{t+1}(k+n), & x_{t+1}(k+n+1), & 1,\ldots)
\end{array}
\tag{17}
$$

Loosely speaking, as the time increases from t to $t+1$, the state has not propagated in case (a), it has advanced to the right by one site in case (b) and it has propagated with dispersion in case (c).

To decide among these possibilities, one needs to investigate the value of f_- and f_+ at the boundary sites $i = k+1$ and $i = k+n$, respectively. Letting

$$
\gamma_- = \frac{a(\varepsilon - a)}{1-\varepsilon} \qquad \gamma_+ = \frac{a(a+\varepsilon-1)}{\varepsilon}
$$

one verifies that the functions $f_\pm$ satisfies the following equations

$$
\begin{array}{ll}
f_-(-a) = -1 & f_+(-a) = 1-2\varepsilon \\
f_-(a) = 1-2\varepsilon & f_+(a) = 1 \\
f_-(\gamma_-) = -a & f_+(\gamma_+) = a.
\end{array}
\tag{18}
$$

We define the *gap* of the CML with local map f_a to be the open interval $\Gamma = (\gamma_+, \gamma_-)$. Its length (with sign) is given by

$$
\gamma(\varepsilon, a) \;=\; \gamma_- - \gamma_+ \;=\; \frac{a(1-a-2\varepsilon(1-\varepsilon))}{\varepsilon(1-\varepsilon)}. \tag{19}
$$

Let $x \in U$. Then $f_+(x) \in U$ if $x \leq \gamma_+$, and $f_-(x) \in U$ if $x \geq \gamma_-$. From this and the fact that $x_t(i)$ is a non-decreasing function of i we obtain that the size of a step state of minimal mass cannot increase, unless it is zero, for a gap of non-negative size.

In particular, it is not difficult to prove that when the gap size is non-negative, if the size is not greater than 1 at time 0, then it will remain so for all times. A *minimal state* is a minimal mass step state of size 0 or 1. Therefore, if we start with a minimal state, the configuration of the CML will remain a minimal state at any time.

4. SYMBOLIC DYNAMICS OF MINIMAL STATES

We develop a symbolic description of the dynamics of minimal states in the case of non-negative gap length. Their dynamics can be reduced to the iteration of a one-dimensional piecewise linear circle map — the auxiliary map.

1. The auxiliary map

Without loss of generality, we consider minimal states of the form

$$
X_t = (\ldots,-1,-1,x_t(i),1,1,\ldots), \tag{20}
$$

where either $|x_t(i)| \leq a$ or $x_t(i) = -1$, for which we introduce the shorthand notation

$$
X_t = [x,i]_t,
$$

(the subscript t will often be dropped). Thus $[-1,i] = P(i)$ — cf. (9). The image of X_t is given by

$$
X_{t+1} = (\ldots,-1,-1,f_-(x_t(i)),f_+(x_t(i)),1,\ldots). \tag{21}
$$

We define

$$
\varepsilon_c = \frac{1-a}{2} \tag{22}
$$

and note that ε_c is the area enclosed between the graph of f_a and the diagonal, for $x^* < x < x^*_+$. The following two results characterize completely the evolution of X_t in the parameter ranges $\varepsilon \leq \varepsilon_c$ and $\varepsilon \geq 1-\varepsilon_c$.

Theorem 2. *Let X_t be a minimal state of the form* (20)*, and let*

$$
x_- = \frac{\varepsilon a}{1-\varepsilon-a} \qquad x_+ = \frac{a(1-\varepsilon)}{a-\varepsilon}. \tag{23}
$$

(i) If $\varepsilon \leq \varepsilon_c$, then for $x(i) < x_-$ ($x(i) > x_-$) the state $[x,i]$ reaches $P(i)$ ($P(i-1)$) in a finite time. The state $[x_-,i]$ is fixed and unstable.

(ii) If $\varepsilon \geq 1-\varepsilon_c$, then for $x(i) < x_+$ ($x(i) > x_+$) the state $[x,i]$ reaches $P(i+k)$ ($P(i+k-1)$) in a finite time. The state $[x_+,i]$ is fixed and unstable under $G \circ F$, where G is the shift mapping (3).

The proof of the above results is given in appendix B. From Theorem 2 it follows that the velocity of the travelling interface satisfies

$$
v(\varepsilon) = \begin{cases} 0 & \text{if} \quad 0 \leq \varepsilon \leq \varepsilon_c \\ 1 & \text{if} \quad 1-\varepsilon_c \leq \varepsilon \leq 1. \end{cases} \tag{24}
$$

As a consequence, we have that if $\varepsilon \leq \varepsilon_c$ then $F(P(i)) \sim P(i)$, and if $\varepsilon \geq 1-\varepsilon_c$ then $F(P(i)) \sim P(i+1)$. In the rest of this chapter we shall assume that $\varepsilon_c < \varepsilon < 1-\varepsilon_c$.

We partition U into three intervals, namely

$$\begin{aligned} U_+ &= \{x : -a \leq x \leq \gamma_+\} \\ \Gamma &= \{x : \gamma_+ < x < \gamma_-\} \\ U_- &= \{x : \gamma_- \leq x \leq a\}. \end{aligned}$$

Because we are assuming the gap length to be non-negative, we are dealing with a minimal state and then the three possibilities for the state (21) are:

$$\begin{array}{llll} (a) & x_t \in U_- & \Rightarrow & f_-(x_t) \in U,\ f_+(x_t) \in S_+ \\ (b') & x_t \in \Gamma & \Rightarrow & f_-(x_t) \in S_-,\ f_+(x_t) \in S_+ \\ (b) & x_t \in U_+ & \Rightarrow & f_-(x_t) \in S_-,\ f_+(x_t) \in U. \end{array} \tag{25}$$

corresponding to the reduced states — see (17)

$$\begin{array}{ll} (a) & X_{t+1} = (\ldots,-1,-1,x_{t+1},\ 1,\ 1,\ldots) \\ (b') & X_{t+1} = (\ldots,-1,-1,\ -1,\ \ 1,\ 1,\ldots) \\ (b) & X_{t+1} = (\ldots,-1,-1,\ -1,\ x_{t+1},1,\ldots) \end{array}$$

For the case (b') we have the evolution

$$[x,i]_t \longrightarrow [-1,i]_{t+1} \longrightarrow [1-2\varepsilon, i+1]_{t+2}. \tag{26}$$

All possibilities are accounted for by defining the *auxiliary map* $\Phi_{\varepsilon,a}$ to be the 2-parameter map (see figure 3)

$$\Phi_{\varepsilon,a}(x) = \begin{cases} f_+(x) & \text{if } x \in U_+ \\ 1-2\varepsilon & \text{if } x \in \Gamma \\ f_-(x) & \text{if } x \in U_- \end{cases} \qquad \varepsilon_c < \varepsilon < 1-\varepsilon_c. \tag{27}$$

It is plain that $\Phi_{\varepsilon,a}$ maps U onto itself and if, in addition, γ is positive, then U_-, Γ and U_+ have positive measure. This characterizes the domain and range of $\Phi_{\varepsilon,a}$.

The auxiliary map reduces the dimensionality of our system. Originally the CML is an infinite dimensional system since it has an infinite number of sites. But in the case of minimal states the dynamics of the whole lattice is reduced to that of the auxiliary map $\Phi_{\varepsilon,a}$, as illustrated schematically in figure 4. Iterating the CML q times amounts to applying the auxiliary map q times on the interface site. During these q iterations, whenever the branch f_- is used the interface is not shifted; whenever f_+ is applied we shift the interface by one site to the right; and finally, when the interface site falls into Γ the CML essentially undergoes two iterations — cf. (26) — but the final result is that the interface site value is $1-2\varepsilon$ as well as being shifted one site to the right.

2. Symbolic dynamics

The following binary symbolic dynamics for the auxiliary mapping $\Phi_{\varepsilon,a}$ will play a decisive role in the rest of the paper.

We assign the symbols '0' to U_-, the symbol '1' to U_+, and the symbol '10' to Γ. This choice originates from the prescriptions (25), according to which the location of a minimal state remains unchanged for $x \in U_-$, increases by one for $x \in U_+$, and increases by one for every two iterations for $x \in \Gamma$. To the orbit of the auxiliary mapping with initial condition x we associate the semi-infinite sequence of symbols

$$S = S(x) = (s_1, s_2, s_3, \ldots) \qquad s_k \in \{0,1\}$$

where we stipulate that the symbol '10' generates two binary symbols: '10'$\longrightarrow$'1','0'. For this reason, our code will not be unique. The space of binary sequences is denoted by Σ_2, and is equipped with the usual topology.

Any orbit with an element in Γ will be called a *gap orbit*. If this orbit is periodic, then the period of its symbolic representation is one greater than that of the orbit, because the gap Γ corresponds to two symbols.

The *rotation number* [13,14] of the orbit through x is defined as

$$\nu = \lim_{T\to\infty} \frac{1}{T} \sum_{t=0}^{T} s_t \tag{28}$$

provided that the limit exists. If this is the case, it is plain that $0 \leq \nu \leq 1$.

We will show that the symbol sequence $S(x)$ can be characterized in terms the *spectrum* of ν, which is defined as the following sequence of integers

$$Spec(\nu) = \lfloor \nu \rfloor, \lfloor 2\nu \rfloor, \lfloor 3\nu \rfloor, \ldots = a_1, a_2, a_3, \ldots \tag{29}$$

where $\lfloor\cdot\rfloor$ is the floor function. Because $0 \leq \nu \leq 1$, consecutive elements of $Spec(\nu)$ differ by zero or one. Thus defining

$$\tau(a_1, a_2, \ldots) = (a_2 - a_1, a_3 - a_2, \ldots),$$

we find that $\tau(Spec(\nu))$ is a binary sequence.

Using symbolic dynamics it is easy to follow the evolution of the minimal state: every iteration corresponds to a new symbol in the sequence. If the symbol is '0' then the minimal state remains in the same place and if the symbol is '1' the minimal state is shifted one site to the right. We can assume the velocity of the travelling front to be constant, so that the spectrum of the velocity gives the position of the minimal state at every iteration, since the location of the minimal state can only take integer values. Thus τ applied on $Spec(\nu)$ gives a 0 when the position of the minimal state remains unchanged and a 1 when it jumps from on site to its right neighbour. Therefore the symbolic binary sequence associated to a given rotation number ν can be computed as

$$S = \tau\left(Spec(\nu)\right). \tag{30}$$

If ν is rational, then $\tau(Spec(\nu))$ is periodic, as easily verified. For example, the sequence $S(3/7)$ is given by

$$\begin{aligned} S(3/7) &= \tau\left(Spec(3/7)\right) \\ &= \tau(0,0,1,1,2,2,3,3,\ldots) \\ &= (\overline{0,1,0,1,0,1,0}), \end{aligned}$$

where the bar denotes periodicity.

The symbolic dynamics of $\Phi_{\varepsilon,a}$ is that of a uniform rotation with rotation number ν analogous to that of a subcritical circle map, as we shall see later. The dynamics of the whole lattice is then reduced to the study of the one-dimensional map $\Phi_{\varepsilon,a}$ whose rotation number gives the velocity of propagation of the travelling front. Using arguments similar to that given in section 1.14 of [15], it is possible to prove that the rotation number is a well-defined, non-decreasing, continuous function of the parameters (ε, a) and it is independent of the initial condition. The difference here is that the auxiliary map is a non-decreasing function and not a strictly increasing one as in [15], but the same line of proof may be followed. Therefore, when the gap size is non-negative, the velocity $v(\varepsilon)$ of the travelling interface is a well defined, non-decreasing, continuous function and does not depend on the choice of the initial minimal state.

5. STRUCTURE OF PARAMETER SPACE

We now turn to the study of the parameter space of the coupled map lattice $F_{\varepsilon,a}$, in the case where the gap size $\gamma(\varepsilon,a)$ is non-negative (cf. (19)). Then the gap orbit is defined, and we denote by $v = v(\varepsilon, a)$ the velocity of the center of mass of the corresponding minimal state.

1. Mode-Locking

Using the symbolic coding we now prove that the gap Γ forces the velocity of the travelling wave to be locked to rational values if $\Phi_{\varepsilon,a}$ has an eventually periodic orbit containing the point $1-2\varepsilon$. Mode-locking guarantees stability of the propagating signal with respect to parametric perturbations.

The symbolic coding of the orbit of the auxiliary map $\Phi_{\varepsilon,a}$ gives the velocity of the travelling interface via the rotation number (28). The presence of a non-negative gap Γ induces a mode-locking of the rotation number in the following way. Let us consider the orbit generated from an arbitrary point x_0 in Γ. If after q iterations x_q falls into Γ, the orbit is eventually periodic [15] of period q with rotation number p/q, $p-1$ being the number of times the orbit visits U_+ (recall that there is an extra symbol '1' coming from the gap).

Suppose now that we introduce a small perturbation of the parameters and the initial condition: $(x_0, \varepsilon, a) \longrightarrow (x_0', \varepsilon', a')$. The perturbed orbit $x_t' = \Phi^t_{\varepsilon',a'}(x_0')$ is initially at a distance $\Delta x_0 = x_0' - x_0$ from the unperturbed one. Using the continuity of x_t' on the parameters ε, a and the initial condition, the distance Δx_t between the two orbits at time t can be made as small as we want by making (x_0, ε, a) sufficiently close to (x_0', ε', a'). Because Γ is an open interval, if x_q belongs to Γ, then so does x_q' for a sufficiently small perturbation. Therefore we have established the crucial result:

Theorem 3. *If the gap orbit of $\Phi_{\varepsilon,a}$ is finite, then it is stable under a sufficiently small perturbation of parameters and initial condition.*

Thus there is a region in the parameter space (ε, a), where the given rotation number is constant or *mode-locked*. An example of mode-locking ε-regions for a fixed value of a is given in figure 1. The mode-locked region, corresponding to a given rotation number $\nu = p/q$, can be computed by noting that in order that an orbit through any point in Γ returns after $q-1$ iterations we must have that $\Phi^{q-1}_{\varepsilon,a}(\Gamma) \subseteq \Gamma$. This condition may be rewritten as $\Phi^{q-2}_{\varepsilon,a}(1-2\varepsilon) \in \Gamma$ giving the inequalities

$$\gamma_+ \quad \leq \quad \Phi^{q-2}_{\varepsilon,a}(1-2\varepsilon) \quad \leq \quad \gamma_-, \tag{31}$$

since

$$\forall\, x_0 \in \Gamma \quad \Longrightarrow \quad x_1 = \Phi_{\varepsilon,a}(x_0) = 1 - 2\varepsilon.$$

We shall mention that the end points of (31) are included because an orbit arriving at $\gamma_\pm$ after $q-2$ iterations will also reach $1-2\varepsilon$ after two more iterations since $\Phi_{\varepsilon,a}\left(f_\pm(\gamma_\pm)\right) = \Phi_{\varepsilon,a}(\pm a) = 1-2\varepsilon$ (cf. (18)) — these two orbits correspond to the kneading sequences of the local map [16,17]. The closed ε-interval region for which the velocity is mode-locked to a given rational is called a *plateau*.

Equation (31) ensures that the orbit starting at $x_1 = 1-2\varepsilon$ falls into the gap after $q-2$ iterations and therefore repeats itself after $q-1$ iterations. The value of $\Phi^{q-2}_{\varepsilon,a}(1-2\varepsilon)$ is determined by the coding sequence of the associated rotation number. So if we want to compute the mode-locked region for a given velocity $\nu = p/q$ we have to determine the (ε, a) region where (31) is satisfied in correspondence to the code $S(p/q)$ given by (30). For example, to compute the mode-locked region for the velocity $\nu = 2/5$ we first compute $S(2/5) = (\overline{0,1,0,1,0})$, so we know that the orbit visits the regions U_-, U_+, U_- and Γ. Solving for $\Phi^3_{\varepsilon,a}(1-2\varepsilon) = f_-\left(f_+\left(f_-(1-2\varepsilon)\right)\right)$ gives

$$\gamma_+ \quad \leq \quad f_-\left(f_+\left(f_-(1-2\varepsilon)\right)\right) \quad \leq \quad \gamma_-.$$

In figure 5 we show the mode-locking regions in the (ε, a)-plane, computed via (31), for some rational velocities. These regions, represented as shaded areas, are the so-called *Arnold's tongues* [14,18]. It can be observed that as we approach the zero-gap line (dashed line) — given by $\gamma = 0$ in (19) — the tongue size decreases, as the latter is related to the gap size.

2. Lattice representation

We now introduce a geometric representation of the rational velocities of the wavefront. This representation gives a straightforward method for computing the associated coding sequence as well as some properties related to the mediant of two given consecutive rational velocities of a Farey sequence.

We represent the rational velocity $v = m/n$ as the point $P(m/n) = (n-m, m)$ on the integral lattice $\mathbb{Z}^2$. Consider the ray *OP* emanating from the origin and passing through $P(m/n)$. It is obvious that distinct irreducible rational velocities correspond to distinct points and distinct rays. The ray *OP* will intersect the lattice grid infinitely many times. We drop the first intersection in O and take all the remaining ones. Next, write a '0' every time the ray *OP* crosses a vertical grid line, write a '1' when it crosses a horizontal grid line and write '10' when its crosses through a lattice point (see example in figure 6). The resulting semi-infinite binary sequence can be shown to be equal to the symbolic coding of the velocity $\nu = m/n$ given by (30).

We sketch the proof. Recall that a '0' in $S(m/n)$ means one iteration of the CML without advance of the interface while a '1' means that the interface has advanced one site. Let us now consider the consequence of crossing vertically and horizontally the grid lines of $\mathbb{Z}^2$. Crossing a vertical line of the grid means transition from the point $(n-m, m)$ to the point $(n+1-m, m)$, *i.e.* from $P(m/n)$ to $P(m/(n+1))$ — this corresponds to iterating the CML once without any advance of the interface (symbol '0'). Crossing a horizontal line means moving from the point $(n-m, m)$ to the point $(n-m, m+1) = ((n+1)-(m+1), m+1)$, *i.e.* from $P(m/n)$ to $P((m+1)/(n+1))$, which corresponds to a shift of one site of the interface after one iteration (symbol '1'). And finally, crossing through a lattice point is equivalent to a shift of one place of the interface in two iterations (symbol '10').

We recall that the Farey series [19,20] of order r, $\mathfrak{F}_r$, is defined to be the set of irreducible fractions, in ascending order, belonging to $[0,1]$ whose denominators are smaller than or equal to r. Suppose now that the velocities $v = m/n$ and $v' = m'/n'$ are two consecutive rationals of the Farey series $\mathfrak{F}_{\max(n,n')}$. Then, using the lattice representation, it is not difficult to see that if $m/n < m'/n'$ the coding sequence of the velocity $v'' = (m+m')/(n+n')$ corresponding to their *mediant* is given by

$$S\left(\frac{m+m'}{n+n'}\right) = S\left(\frac{m}{n}\right) S\left(\frac{m'}{n'}\right), \tag{32}$$

where the right hand side denotes the *concatenation* of two periodic sequences, defined as follows. If $S_a = (\overline{a_1, \ldots, a_p})$ and $S_b = (\overline{b_1, \ldots, b_q})$ are periodic sequences of period p and q, respectively, their concatenation $S_a S_b$ is the periodic sequence of period $p+q$ defined as

$$S_a S_b = (\overline{a_1, \ldots, a_p, b_1, \ldots, b_q}). \tag{33}$$

The result (32) derives from the fact that the parallelogram $(OPP''P')$, with $P = P(m/n), P' = P'(m'/n')$ and $P'' = P''(m''/n'') = P''((m+m')/(n+n'))$, does not contain any lattice point since m/n and m'/n' are consecutive numbers of a Farey series [20].

An example of this construction is shown in figure 6 where the velocities $v = 1/3$ and $v' = 1/2$ give the mediant $v'' = 2/5$. The sequence for $v = 1/3$ is $(\overline{010})$ (vertical cross + lattice point) and the sequence for $v' = 1/2$ is $(\overline{10})$ (just a lattice point) and the resulting sequence for the mediant $(\overline{01010})$ is obtained by the concatenation $(\overline{010})(\overline{10})$.

3. Unimodular transformations and envelopes

The structure of the parameter space of the mapping $F_{\varepsilon,a}$ at the boundary of a tongue can be described analytically by means of *envelopes*. These are functions characterizing the structure of sequences of adjacent tongues. The study of envelopes proceeds in two stages. Firstly we derive upper and lower envelopes for the so-called first order plateaus (*i.e.* $v = 1/n$ and $v = (n-1)/n$, $n = 1, 2, \ldots$). Then with the use of unimodular transformations we find envelopes for any family of plateaus.

The *zeroth order plateaus* are defined as the two plateaus given by (24) with velocities $\{0/1, 1/1\}$. In order to construct any order of plateaus, the *k-th order plateaus*, we take any two consecutive elements of the previous order $k-1$ denoted by $v_a = m_a/n_a$ and $v_b = m_b/n_b$ $(v_a < v_b)$. Then the next order of plateaus is defined as the following infinite increasing sequence of mediants

$$\left\{\ldots, \frac{3m_a+m_b}{3n_a+n_b}, \frac{2m_a+m_b}{2n_a+n_b}, \frac{m_a+m_b}{n_a+n_b}, \frac{m_a+2m_b}{n_a+2n_b}, \ldots\right\} \tag{34}$$

The first order plateaus are thus given by

$$\left\{\ldots, \frac{1}{4}, \frac{1}{3}, \frac{1}{2}, \frac{2}{3}, \frac{3}{4}, \ldots\right\}.$$

They form an unique family. On the other hand, between any two consecutive plateaus of a given order there is a new family of plateaus of the next order and so on. This construction is similar to that of the Farey series [19]. In particular, any two consecutive plateaus p/q and p'/q' ($p/q < p'/q'$) of the same order and family are consecutive fractions of a Farey series (*i.e.* $qp' - pq' = 1$).

From the definition of the sequence of plateaus (34) and by applying repetitively the sequence concatenation (32) it is possible to find the sequences associated to a given family of plateaus:

$$\{\ldots,\, S_a^3 S_b,\, S_a^2 S_b,\, S_a S_b,\, S_a S_b^2,\, S_a S_b^3, \ldots\}\,,$$

where we used the shorthand notation $S_a = S(m_a/n_a)$ and $S_b = S(m_b/n_b)$. It will be useful to distinguish the left Σ_a and right Σ_b subfamilies of sequences defined by

$$\begin{aligned}\Sigma_a &= \{\ldots,\, S_a^3 S_b,\, S_a^2 S_b,\, S_a S_b\}\\ \Sigma_b &= \{S_a S_b,\, S_a S_b^2,\, S_a S_b^3, \ldots\}\,.\end{aligned} \tag{35}$$

Note that the sequence $S_a S_b$, corresponding to the mediant of v_a and v_b, appears in both families. The elements of the subfamilies Σ_a (Σ_b) tend, to the left (right), to S_a (S_b). Thus the subfamilies Σ_a (Σ_b) correspond to velocities going from the mediant of v_a and v_b to the plateau v_a (v_b).

From now on we consider only Σ_a. All the results generalize to Σ_b just by interchanging the subscripts a and b. The elements of Σ_a are of the form

$$S \in \Sigma_a \quad\Longrightarrow\quad S = S_a^n S_b \qquad n = 1, 2, \ldots \tag{36}$$

which correspond to the velocities

$$v(S_a^n S_b) = \frac{n\, m_a + m_b}{n\, n_a + n_b} \qquad n = 1, 2, \ldots \tag{37}$$

We recall that the transformations (37) are unimodular since we always deal with consecutive fractions of Farey series.

The sequences S_a and S_b correspond to a particular combination of f_- and f_+. Since $f_\pm$ are linear, any such combination will again give a linear function. We denote by f_{S_a} (f_{S_b}) the linear function resulting from the combination of $f_\pm$ specified by the sequence S_a (S_b):

$$\begin{aligned}f_{S_a}(x) &= \alpha_a x + \beta_a\\ f_{S_b}(x) &= \alpha_b x + \beta_b.\end{aligned} \tag{38}$$

Composing f_{S_a} with itself n times gives

$$f_{S_a}^n(x) = f_{S_a^n}(x) = \alpha_a^n (x - \xi_a^*) + \xi_a^* \tag{39}$$

where $\xi_a^* \equiv \beta_a/(1-\alpha_a)$ is the fixed point of f_{S_a}. Combining (38) and (39) in (36) we obtain the iterates of $x_0 = 1 - 2\varepsilon$ under $\Phi_{\varepsilon,a}$ for the coding sequences $S_a^n S_b$

$$f_{S_a^n S_b}(x_0) = f_{S_b}\left(f_{S_a}^n(x_0)\right)\,. \tag{40}$$

Replacing (40) in (31) we obtain the mode-locking region for a given series of plateaus

$$f_{10}(\gamma_+) \quad\leq\quad \alpha_b(\alpha_a^n(x_0 - \xi_a^*) + \xi_a^*) + \beta_b \quad\leq\quad f_{10}(\gamma_-), \tag{41}$$

where we have taken into account the fact that the two final symbols '10' of any sequence in Σ_a come from the gap Γ and therefore they have to be compensated by replacing $\gamma_\pm$ in (31) by $f_1(f_0(\gamma_\pm)) = f_{10}(\gamma_\pm)$.

As we mentioned earlier, the plateaus include their end points. These are obtained from solving the inequalities (41) for the extremes $f_{10}(\gamma_\pm)$. Therefore, all the end points of a given family of plateaus are given by

$$\alpha_b(\alpha_a^n(x_0 - \xi_a^*) + \xi_a^*) + \beta_b = f_{10}(\gamma_\pm), \tag{42}$$

where the positive (negative) sign gives the left (right) end points of the plateaus. As we vary $n = 0, 1, \ldots$ in (42) we browse all the extremes of the series of plateaus going from the mediant of v_a and v_b to v_a.

Solving (42) for n yields

$$n_\pm(\varepsilon, a) = \frac{1}{\ln \alpha_a}\,\ln \frac{f_{10}(\gamma_\pm) - \beta_b - \alpha_b \xi_a^*}{\alpha_b(x_0 - \xi_a^*)}.$$

Finally, replacing the value of n in (37) by $n_\pm(\varepsilon, a)$ gives the continuous functions

$$v_\pm(\varepsilon, a) = \frac{n_\pm(\varepsilon, a)\, m_a + m_b}{n_\pm(\varepsilon, a)\, n_a + n_b}, \tag{43}$$

that passes through all the left (v_+) and right (v_-) boundaries of the plateaus. Therefore, $v_\pm$ gives the upper ($+$) and lower ($-$) envelopes of the series of plateaus (37).

In figure 7a we display the first order plateaus for $a = 0.4$. We only plotted the left family ($v \leq 1/2$) since the right family ($v \geq 1/2$) is symmetrical from (11). An example of a second order family, for the same value of a, is shown in figure 7b where we display the lower and upper envelopes for the left and right families of second order plateaus between $v = 1/2$ and $v = 1/3$.

With the method described above, it is possible to find the envelopes of any sequence of high order plateaus via unimodular transformations. The self-similarity structure of the velocity function, easily observable in figures 7a and 7b, is controlled by modular transformations (37) and envelopes. Since it is possible to find a periodic symbolic sequence for any given rational velocity arising from an eventually periodic orbit of $\Phi_{\varepsilon,a}$ through $1 - 2\varepsilon$ then it is possible to find a non-empty ε interval where the velocity is mode-locked (Theorem 3). Therefore the graph of the velocity $v(\varepsilon, a)$ as a function of ε is in fact a *Devil's staircase* [18,21], *i.e.* a fractal staircase. This mode-locking phenomenon is very similar to the one observed for a uniform rotation in a subcritical perturbed circle map [14].

If, on the other hand, the symbolic sequence is chosen to be non periodic, the associated velocity ν is irrational. The continuity of the function $v(\varepsilon)$ guarantees that there exists at least one value of ε such that $v(\varepsilon) = \nu$. We believe that it is possible to prove that there is only one such ε. The idea is to take a sequence of rational approximants of ν; the corresponding upper and lower envelopes should approach each other, as the approximants tend to ν, and coincide in the limit to give a unique ε such that $v(\varepsilon) = \nu$.

4. Convergence to minimal states

In this chapter we have described the structure of the parameter space associated with minimal states. Here we generalize the notion of minimal state and briefly complete our description of the parameter space.

A minimal state — a step state of size 0 or 1 — is stable under iteration when the gap is non-negative. When the gap is negative, the stable configuration of a step state is found to have size assuming only two values, N and $N-1$. Such states will be called minimal N-states.

Numerical experimentation reveals that the integer N does not depend on the initial condition. Any initial configuration we have tried in the interface (increasing, decreasing, oscillatory, random with small and large size, etc ...) converged, after a transient (depending on the initial conditions) to a minimal N-state, with the value of N depending only on ε and a. Accordingly, the parameter space is partitioned into layers where the value of N is constant, as depicted in figure 8. The boundary between the first layer (minimal 1-state) and the second one (minimal 2-state) is the zero-gap curve, given by $\gamma = 0$ in (19). Above that curve the gap is negative, and there appears to be an infinite family of layers labeled by the value of N, separated by boundary curves which may not be differentiable.

The dynamical analysis for such minimal N-states may be carried out by reducing the dynamics of the whole lattice to a N-dimensional auxiliary map [22] analogous to the one obtained previously for minimal 1-states.

6. GENERALIZATIONS AND CONCLUSIONS

We have described a mechanism that allows travelling interfaces in a one-way CML (5) for a special family of piece-wise linear maps (12). We now give some ideas on the generalization of these results to a broader range of functions and couplings.

First of all, the superattractiveness of the points x_-^* and x_+^* is not necessary. It suffices that the map f be a contraction mapping at $x_\pm^*$. This is the case, for instance, if $f''(x) < 0$ for $x_-^* < x < x^*$ and $f''(x) > 0$ for $x^* < x < x_+^*$, where x^* is the unstable fixed point in between x_-^* and x_+^*. However, without superattractiveness, the travelling wave will be less stable to perturbations. Then, if we are dealing with a medium involving random fluctuations we would like the map to be sufficiently contracting for a travelling interface to survive. On the other hand, the lack of superstability of $x_\pm^*$ introduces more sites in the interface since the convergence to $x_\pm^*$ is slower. Moreover, in this case the number of sites contained in the open interval (x_-^*, x_+^*) is not necessarily finite (take the example of an exponentially localized state). For this reason the reduction of the dynamics in this case does not lead to any simplification. Nevertheless, if the shape of the front remains unchanged during the evolution, it is possible to concentrate our attention to a single site in the interface since the remaining sites are determined by the shape of the front. We could, for example, consider the site that is closest to the unstable point x^* and from it reconstruct a one-dimensional auxiliary map that accounts for the whole dynamics, in the same way that $\Phi_{\varepsilon,a}$ accounts for the whole dynamics of minimal states. A more detailed study will be given in [22].

Secondly, the discontinuity of the derivative of the local map is not necessary for mode-locking. We have observed mode-locking for analytic maps as well. In figure 9 a window of the velocity as a function of ε is shown for some polynomials maps (of odd degrees from 5 to 13). The plateaus $v = 1/2$ and $v = 1/3$ are clearly visible. The origin of mode-locking is not related to non-analyticity. It ultimately lies with the asymptotic ($t \to \infty$) discontinuity from the initial conditions associated with the repelling fixed point x^* between the two stable points, which separates two dynamical behaviours.

In this respect the value of the derivative at the repeller can be interpreted as a measure of this discontinuity. It is therefore expected that, for fixed value of the derivative at the attractors, the mode-locked plateaus become more pronounced as the derivative at the repeller point increases. In figure 9 the plateaus $v = 1/2$ and $v = 1/3$ are almost imperceptible for the polynomial of degree 5 that has a derivative at the repelling point $\sim$1.9, meanwhile they become more appreciable for the polynomials of higher degree (7, 9, 11 and 13) where the derivative at the repelling point gets larger ($\sim$2.2, 2.5, 2.7 and 2.9 respectively).

Finally, the travelling wave property arises from one-way coupling in the CML and the direction of the wave is given by that of the coupling. By comparison, a front on a diffusive CML (4) with a symmetric map at each site is going to remain stationary in the long term. For the front to advance one needs asymmetry, either on the coupling or in the local map (with respect to the repeller point x^*) which generates a bias between competing attractors.

In order to illustrate this phenomenon let us take the logistic map $f_\mu(x) = \mu x(1-x)$. The logistic map itself does not fulfill the requirements (two attractive points with a repeller in between) but consider its second iterate f_μ^2. At the parameter value $\mu = 1+\sqrt{5}$ the mapping f^2 has two superattractive fixed points $x_-^* = 1/2$ and $x_+^* = 1/2 + \sqrt{2}\sqrt{3-\sqrt{5}}/4)$ (corresponding to a superattractive 2-cycle for f) separated by a repeller $x^* = 1-\sqrt{2}\sqrt{3-\sqrt{5}}/4$. Consider iterating the diffusive CML with the map f_μ^2 at each site. For an initial step state we obtain a travelling interface where the velocity again behaves as in the examples shown above — it has a transition from $v(\varepsilon) = 0$ to $v(\varepsilon) > 0$ at $\varepsilon_c \simeq 0.198$ —, see figure 10. In this case the mode-locking is not apparent at first glance. However, on amplification, the plateaus are shown to occur. For example, the plateaus corresponding to $v = 1/7$ (right) and $v = 1/8$ (left) are shown in the enlargements in figure 10.

In conclusion, the mode-locking of the velocity of the travelling interface, appears to be an universal phenomenon in coupled map lattices. It implies that waves travelling with rational velocities are stable under both spatial and parametric perturbations.

Appendix A

In this appendix we provide various statements and proofs concerning the image of localized states.

Lemma A.1. *Let X_t be a localized state of a one-way CML, let $x_\pm = \lim_{i\to\pm\infty} x_t(i)$, and let $M(X_{t+1}) \neq 0$. Then, if f is bounded and continuous at $x_\pm$, X_{t+1} is a localized state. If, in addition, X_t is exponentially localized, so is X_{t+1}.*

Proof. We begin considering the case $i \to \infty$. Because X_t is localized, x_+ is finite. Moreover, since f is continuous at x_+, then there exists a constant $\rho > 0$ and an integer N such that, for all $i \geq N$ we have $|f(x_t(i+1)) - f(x_t(i))| < \rho |x_t(i+1) - x_t(i)|$, whence

$$\begin{aligned}
\Delta x_{t+1}(i) &= |(1-\varepsilon)\, f(x_t(i+1)) + \varepsilon\, f(x_t(i)) \\
&\quad -(1-\varepsilon)\, f(x_t(i)) - \varepsilon\, f(x_t(i-1))| \\
&\leq (1-\varepsilon)\,|f(x_t(i+1)) - f(x_t(i))| \\
&\quad + \varepsilon\,|f(x_t(i)) - f(x_t(i-1))| \\
&< \rho\,(1-\varepsilon)\,|x_t(i+1) - x_t(i)| \\
&\quad + \rho\varepsilon\,|x_t(i) - x_t(i-1)| \\
&= \rho\,(1-\varepsilon)\,\Delta x_t(i) + \rho\varepsilon\Delta x_t(i-1), \quad i > N.
\end{aligned} \tag{A.1}$$

Then, from absolute convergence

$$\begin{aligned}
\textstyle\sum_{i=N+1}^{\infty} \Delta x_{t+1}(i) &< \rho(1-\varepsilon) \textstyle\sum_{i=N+1}^{\infty} \Delta x_t(i) \\
&\quad + \rho\varepsilon \textstyle\sum_{i=N+1}^{\infty} \Delta x_t(i-1) < \infty.
\end{aligned}$$

A similar inequality holds for $i \to -\infty$. From the above and the fact that any finite sum of $\Delta x_{t+1}(i)$ is bounded (because f is bounded) it follows that M_{t+1} is finite (and non-zero, by hypothesis), so that the probability p_{t+1} exists. Finally, multiplying both sides of the inequality (A.1) by i and by i^2, respectively, and summing over $i > N$ shows that μ_{t+1} and σ_{t+1} are finite, whence X_{t+1} is localized.

If X_t is exponentially localized, then there exist positive constants c and $\kappa < 1$ for which

$$\Delta x_t(i) < c\kappa^i. \tag{A.2}$$

Combining the above with (A.1) we obtain

$$\Delta x_{t+1}(i) \;<\; \kappa^i c\rho\left((1-\varepsilon) + \frac{\varepsilon}{\kappa}\right), \qquad i > N. \tag{A.3}$$

A similar estimate holds for negative i, showing that X_{t+1} is exponentially localized (possibly with a larger constant c). □

From Lemma A.1 and the fact that the mass of a step state is bounded from (cf. (8)) we obtain immediately

Corollary A.2. *Let X_t be a step state of a one-way CML, and let f be continuous at $x_\pm^*$ and bounded. Then X_{t+1} is a step state. If, in addition, X_t is exponentially localized, so is X_{t+1}.*

We have then establish the invariance of the localized and exponentially localized states under the dynamics of the CML and we are ready now to give a proof for Theorem 1.

Theorem 1. *Let X_0 be an exponentially localized step state of a one-way CML. Let the local map f be bounded, and let f be a contraction mapping in a neighbourhood of the fixed points* (7)*. Then, for all sufficiently small ε, $v(\varepsilon) = 0$ and $v(1-\varepsilon) = 1$, independently of X_0.*

Proof. We deal with the case of small coupling first, and positive i. From Corollary A.2 we know that X_t is an exponentially localized step state for all $t \geq 0$. By assumption f is a contraction mapping in some domain $|x - x_+^*| < r$. Let N' be such that for all $i \geq N'$ we have $|x_t(i) - x_+^*| < r/2$, so that $\Delta x_t(i) < r$. Then, for $i \geq N'$, the constant ρ appearing in (A.1) can be chosen to be smaller than 1.

Let N'' be such that $\Delta x_t(i) < 1$ for all $i \geq N''$, and let $N = \max(N', N'')$. Then since X_t is exponentially localized, we can choose κ so that the bound (A.2) holds for $i \geq N$ with $c = 1$. Letting $c = 1$ in (A.3) it follows that

$$\Delta x_{t+1}(i) \;<\; \kappa^i \qquad i > N \tag{A.4}$$

provided that

$$\varepsilon < \frac{\kappa}{\rho}\,\frac{1-\rho}{1-\kappa}$$

which is satisfied for sufficiently small ε, since the right hand side is positive.

It remains to consider the case $i = N$. Because f is bounded, the quantity

$$\Delta f = \sup_x f(x) - \inf_x f(x)$$

is finite. We have, in place of (A.1)

$$\Delta x_{t+1}(N) < \rho\,(1-\varepsilon)\,\Delta x_t(N) + \varepsilon\,\Delta f$$

giving, for all $t \geq 0$

$$\Delta x_{t+1}(N) < \alpha^{t+1}\kappa^N + \varepsilon\,\Delta f\,\frac{1-\alpha^{t+1}}{1-\alpha},$$

where $\alpha = \rho(1-\varepsilon) < 1$. The right-hand side of the above inequality can be made smaller than κ^N for all t, provided that ε is sufficiently small. Thus the inequality (A.4) holds also for $i = N$.

Let i be negative. Assuming that $\Delta x_t(i) < \kappa^{-i}$ for all sufficiently large (negative) i, and proceeding as above, we find that the bound $\Delta x_t(i) < \kappa^{-i}$ for $i \leq -N$ implies that

$$\Delta x_{t+1}(N) < \kappa^{-i}\rho\,(1-\varepsilon+\varepsilon\kappa) < \kappa^{-i}; \qquad i < -N$$

for all ε (all constants have been redefined). The case $i = -N$ gives the recursive inequality

$$\Delta x_{t+1}(-N) < (1-\varepsilon)\,\Delta f + \rho\varepsilon\kappa^{-N+1}$$

which, as before, yields $\Delta x_{t+1}(-N) < \kappa^{-N}$ for sufficiently small ε.

The above induction establishes the time-independent bound

$$\Delta x_t(i) < \kappa^{|i|}, \qquad |i| \geq N, \qquad t \geq 0.$$

for a suitable choice of κ and N, and for all sufficiently small ε. In this ε-range, from the boundedness of f we conclude that $|\mu_t|$ and σ_t are bounded from above for all times. Thus $v(\varepsilon) = 0$, and X_t remains a step state also in the limit $t \to \infty$. □

Appendix B

Proof of Theorem 2.

(i) The dynamics of the i-th site is given by $x_{t+k}(i) = f_-^k(x_t(i))$ since it is coupled to the $(i-1)$-th site whose value is -1. For the dynamics of the $(i+1)$-th site, since $\varepsilon \leq \varepsilon_c$ and $a \leq f_+(x)$ for any $x \in U$, we have that $x_{t+k}(i+1) \in S_+$. Therefore at time $t+k$ the state of the lattice will be equivalent to $X_{t+k} = [f_-^k(x_t), i]$ which depends exclusively on the initial condition $x_t(i)$. If $\varepsilon \leq \varepsilon_c$ the derivative of the map $f_-'(x) = (1-\varepsilon)/a \geq 1$ and then f_- has a repeller at x_-. Therefore $f_-^k(x_t(i))$ will decrease (increase), for $x_t(i) < x_-$ ($x_t(i) > x_-$) until it reaches S_- (S_+) when the state of the lattice is $P(i)$ ($P(i-1)$). For the marginal case $x_t(i) = x_-$ the state of the lattice $X_{t+k} = [f_-^k(x_-), i] = [f_-(x_-), i]$ is fixed and unstable since x_- is an unstable fixed point of f_-.

(ii) Using a similar reasoning, if $\varepsilon \geq 1 - \varepsilon_c$, x_+ is an unstable fixed point of f_+ and the state of the lattice at time $t+k$ is $X_{t+k} = [f_+^k(x_t), i+k]$. Therefore the lattice will reach the state $P(i+k)$ ($P(i+k-1)$) for $x_t(i) < x_+$ ($x_t(i) > x_+$). In the marginal case $x_t(i) = x_+$, the state of the lattice is $X_{t+k} = G^k\left([f_+^k(x_+), i+k]\right) = G^k\left([f_+(x_+), i]\right)$, which is fixed and unstable under $G \circ F$. □

Acknowledgments

RCG would like to thanks DGAPA for financial support during the preparation of this paper and Carmen Cisneros and Alvaro Salas Brito for all their inconditional support.

[1] K. Kaneko, editor. *Theory and applications of coupled map lattices.* John Wiley & Sons, 1993.

[2] E. Atlee Jackson. *Perspective of nonlinear dynamics*, volume 2. Cambridge Univ. Press, 1991. Chap. 10.

[3] K. Kaneko. Spatiotemporal chaos in one- and two-dimensional coupled map lattices. *Physica D*, **37**:60–82, 1989.

[4] D. Keeler and J.D. Farmer. Robust space-time intermitency and $1/f$ noise. *Physica D*, **23**:413–35, 1986.

[5] L.A. Bunimovich, A. Lambert and R. Lima. The emergence of coherent structures in coupled map lattices. *J. Stat. Phys.*, **61**:253, 1990.

[6] L. Ying-Cheng and C. Grebogi. Synchronization of spatiotemporal chaotic systems by feedback control. *Phys. Rev. E*, **50**(3):1894–9, 1994.

[7] R. Kapral and G.-L. Oppo. Competition between stable states in spatially-distributed systems. *Physica D*, **23**:455–63, 1986.

[8] R. Kapral, R. Livi, G.-L. Oppo and A. Politi. Dynamics of complex interfaces. *Phys. Rev. E*, **49**(3):2009–49, 1994.

[9] K. Kaneko. Chaotic travelling waves in a coupled map lattice. *Physica D*, **68**:299–317, 1993.

[10] R.E. Amritkar, P.M. Gade and A.D. Gangal. Stability of periodic orbits of coupled map lattices. *Phys. Rev. A*, **44**(6):3407–10, 1991.

[11] P.M. Gade and R.E. Amritkar. Spatially periodic orbits in coupled map lattices. *Phys. Rev. E*, **47**(1):143–53, 1993.

[12] B. Fernandez. Existence and stability of steady fronts in bistable CML. Preprint, 1995.

[13] J. Stark. Smooth conjugacy and renormalization for diffeomorphisms of the circle. *Nonlinearity*, **1**:541–575, 1988.

[14] G.L. Baker and J.P. Gollub. *Chaotic Dynamics, an introduction.* Cambridge Univ. Press, 1990. Chap. 4.

[15] R.L. Devaney. *An introduction to dynamical systems.* Addison-Wesley, second edition, 1989.

[16] J.H. Hubbard and C.T. Sparrow. The classification of topologically expansive Lorenz maps. *Comm. on Pure and Appl. Maths.*, **43**:431–443, 1990.

[17] P.A. Glendinning and C.T. Sparrow. Prime and renormalisable kneading invariants and the dynamics of expanding Lorenz maps. *Physica D*, **62**:22–50, 1993.

[18] P. Bak. The Devil's staircase. *Physics Today*, December:38–45, 1986.

[19] R.L. Graham, D.E. Knuth and O. Patashnik. *Concrete mathematics, a foundation for computer science.* Addison-Wesley, 1989. Chap. 4.5.

[20] G.H. Hardy and E.M. Wright. *An introduction to the theory of numbers.* Oxford Univ. Press, 4^{th} edition, 1960. Chap. 3.

[21] M. Schroeder. *Fractals, Chaos, Power Laws.* W.H. Freeman and Company, 1991. Chap. 7.

[22] R. Carretero-González, D.K. Arrowsmith and F. Vivaldi. Reduction dynamics for travelling fronts in Coupled Map Lattices. In preparation, 1996.

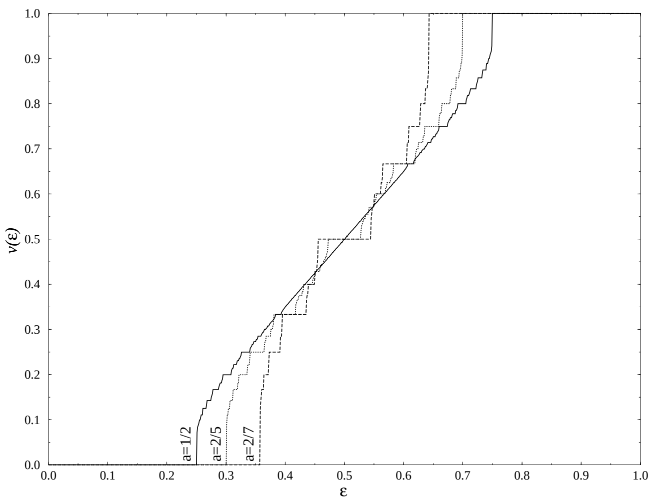

Figure 1: Travelling velocity $v(\epsilon)$ of the interface, for a piece-wise linear one-way couple map lattice as a function of the coupling parameter ϵ, computed numerically for different values of the local map parameter a. The velocity has a staircase-like behaviour symmetric with respect to the point $(\epsilon, v(\epsilon)) = (1/2, 1/2)$.

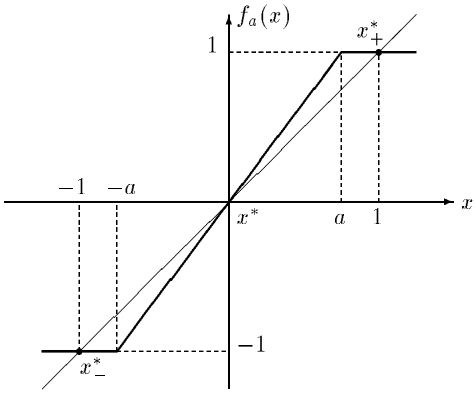

Figure 2: Piece-wise linear local map f_a for the one-way CML.

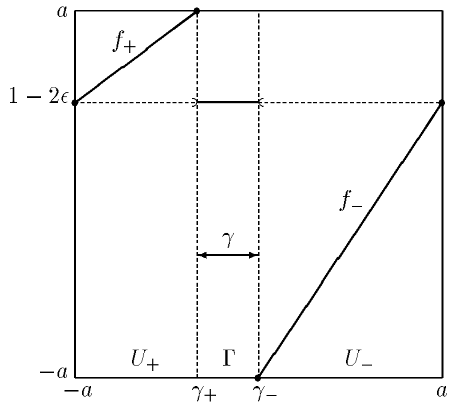

Figure 3: The auxiliary map $\Phi_{\epsilon,a}$ which provides the dynamics of the interface.

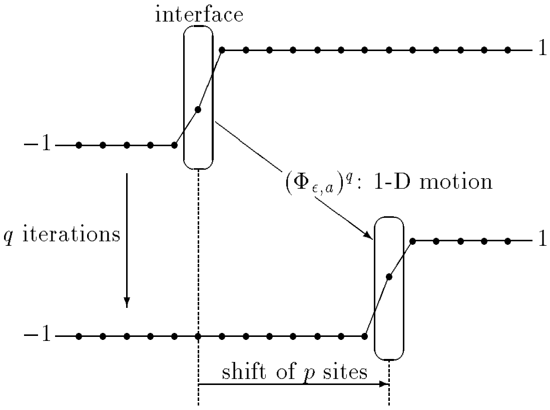

Figure 4: Reduction of the degrees of freedom for minimal states of a one-way CML. The originally infinite-dimensional CML is reduced to a 1-dimensional system. The only degree of freedom is the value of the interface site, its dynamics is being given by the auxiliary map $\Phi_{\epsilon,a}$.

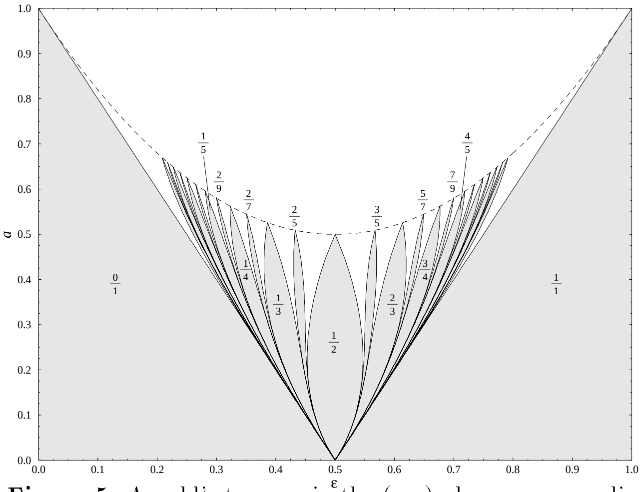

Figure 5: Arnold's tongues in the (ϵ, a)-plane corresponding to rational velocities of the travelling interface for the one-way coupled map lattice $F_{\epsilon,a}$.

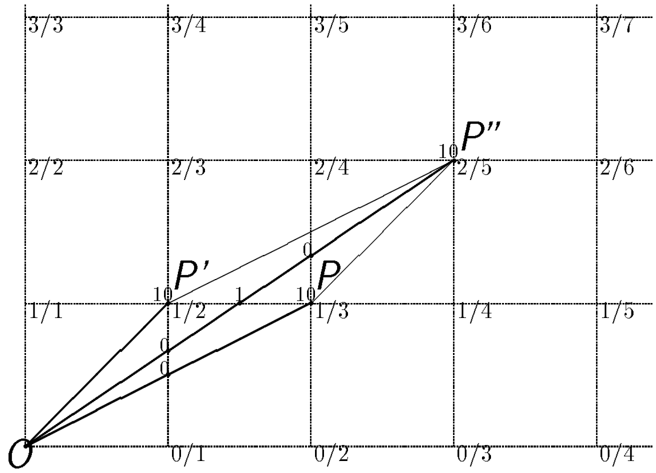

Figure 6: Integral lattice representation of the rational velocities. Every rational velocity m/n corresponds to the point $P(m/n) = (n-m, m)$ on the lattice. Its symbolic sequence is then constructed by the crossings of OP with the grid lines: a '0' corresponds to crossing a vertical line, a '1' a horizontal line and a '10' corresponds to crossing a lattice point. Concatenating sequences for two different velocities m/n and m'/n' corresponds to the vector addition of $OP(m/n)$ and $OP(m'/n')$, and the resulting velocity is the mediant $(m+m')/(n+n')$.

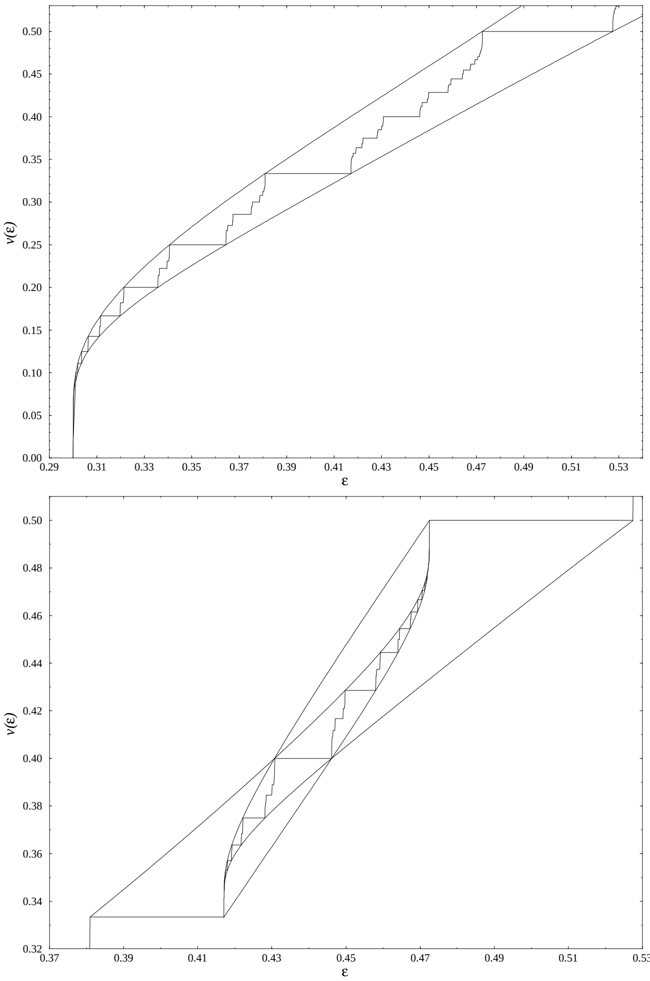

Figure 7: a) Upper and lower envelopes of the first order plateaus for $a = 0.4$. b) Upper and lower envelopes of the second order plateaus between $v(\epsilon) = 1/2$ and $v(\epsilon) = 1/3$.

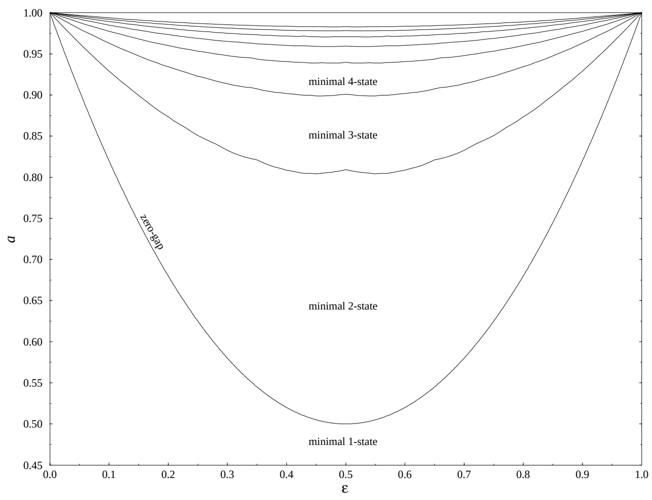

Figure 8: Convergence layers for minimal states in the piecewise liner CML. A N-minimal state is a state with N or $N-1$ sites on the interface. The curve separating the layers 1-minimal state and 2-minimal state is called the zero-gap curve ($\gamma(\epsilon, a) = 0$).

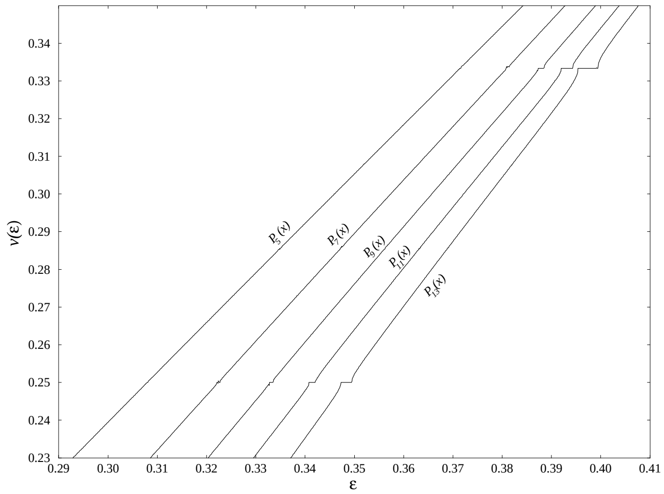

Figure 9: Mode-locking of the velocity for a CML with smooth polynomial local maps P_n. The polynomials P_5, P_7, P_9, P_{11} and P_{13} have degrees 5, 7, 9, 11 and 13 respectively. The plateaus $v = 1/3$ and $v = 1/4$ become increasingly visible with the degree of the polynomials corresponding to increasing the derivative at the origin.

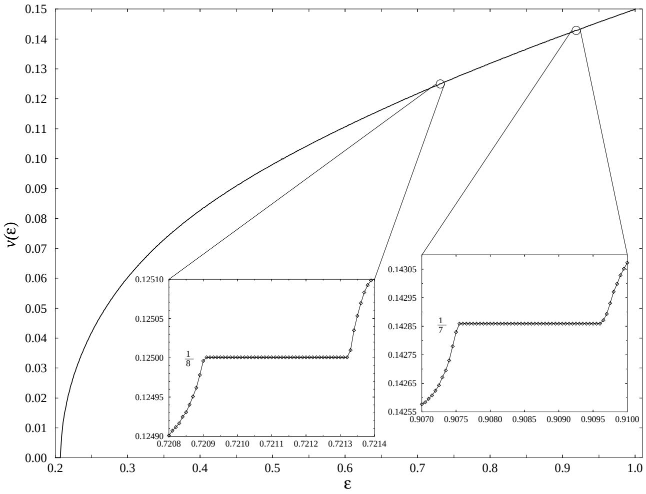

Figure 10: Mode-locking of the velocity of the travelling interface in a diffusive CML. The local map is the second iterate of the logistic map $f_\mu(x) = \mu x(1-x)$ with $\mu = 1 + \sqrt{5}$, and the interface is supported by its two superstable points. The velocity seems to have a smooth graph, but the mode-locking plateaus corresponding to $v = 1/7$ and $v = 1/8$ become evident under magnification.